Preferential Hydrolysis of Aberrant Intermediates by the Type II Thioesterase in *Escherichia coli* Nonribosomal Enterobactin Synthesis: Substrate Specificities and Mutagenic Studies on the Active-Site Residues[†]

Zu-Feng Guo, Yueru Sun, Suilan Zheng, and Zhihong Guo*

Department of Chemistry, Center for Cancer Research, The Hong Kong University of Science and Technology, Clear Water Bay, Kowloon, Hong Kong SAR, China

Received November 24, 2008; Revised Manuscript Received December 31, 2008

ABSTRACT: The type II thioesterase EntH is a hotdog fold protein required for optimal nonribosomal biosynthesis of enterobactin in *Escherichia coli*. Its proposed proofreading activity in the biosynthesis is confirmed by its efficient restoration of enterobactin synthesis blocked in vitro by analogs of the cognate precursor 2,3-dihydroxybenzoate. Steady-state kinetic studies show that EntH recognizes the phosphopantetheine group and the pattern of hydroxylation in the aryl moiety of its thioester substrates. Remarkably, it is able to distinguish aberrant intermediates from the normal one in the enterobactin assembly line by demonstrating at least 10-fold higher catalytic efficiency toward thioesters derived from aberrant aryl precursors without a *para*-hydroxyl group, such as salicylate. By structural comparison and site-directed mutagenesis, the thioesterase is found to possess an active site closely resembling that of the 4-hydroxybenzoyl-CoA thioesterase from *Arthrobacter* sp. strain SU and to involve an acidic residue (glutamate-63) as the catalytic base or nucleophile like all other hotdog thioesterases. In addition, the EntH specificities toward the substrate hydroxylation pattern are found to depend on the active-site histidine-54, threonine-64, serine-67, and methionine-68 with the selectivity significantly reduced or even reversed when they are individually replaced by alanine. These residues are likely responsible for differential interaction of the enzyme with the substrates which leads to distinction between the normal and aberrant precursors in the enterobactin assembly line. These results show that the type II thioesterase evolves its distinctive ability to recognize the aberrant intermediates from the versatile catalytic platform of hotdog proteins and suggests an active search mechanism for type II thioesterases in nonribosomal peptide synthesis.

Nonribosomally synthesized peptide natural products are a large and structurally diverse class of complex molecules that possess a wide range of biological activities. They are assembled by a common thiotemplate mechanism catalyzed by large, modular multifunctional enzymes called nonribosomal peptide synthetases (NRPSs)[1] (*1*−*4*). Each module of these NRPSs contains a set of discrete functional domains responsible for one cycle of peptide chain elongation through activation, modification, and incorporation of one amino acid monomer into the growing peptide chain tethered to the peptidyl carrier protein domain (PCP). The fully elongated polypeptide chain is released or cyclized by a type I thioesterase (TEI) domain covalently linked to the last module of the NRPS (*5, 6*). The gene clusters of many NRPSs are associated with a gene coding a second putative thioesterase (type II thioesterase or TEII), which has been demonstrated to regenerate several NRPS systems whose PCPs are misprimed by acetylation (*7*) or misloaded with noncognate amino acids by the adenylation (A) domain (*8*). This editing activity of TEII is similar to the proofreading activity of ribosomal protein biosynthesis and is important for efficient synthesis of the end peptide product, although it has been proven to be nonessential (*9*−*12*). Due to lack of data showing the ability of the editing enzymes to distinguish between the normal and aberrant intermediates in the peptide assembly lines, a passive proofreading mechanism has been proposed for TEII recognition of the aberrant intermediates by their increased half-lives (*8*), which is similar to the mechanism proposed for recognition of aberrant acyl groups by a TEII associated with polyketide synthases (*13*).

The siderophore enterobactin is a nonribosomal peptide product synthesized from 2,3-dihydroxybenzoate (2,3-DHB) and serine by a two-module NRPS in response to iron deficiency in *Escherichia coli* (*14*). The enterobactin NRPS comprises the 2,3-DHB-AMP ligase EntE, the aryl-carrier protein (ArCP) domain of the bifunctional EntB, and the four-domain protein EntF (Figure 1) (*15*). EntE is responsible for 2,3-DHB activation and aryl transfer to the ArCP (*16, 17*),

[†] This work was financially supported by HKUST and RGC GRF601108 from the Hong Kong SAR government.

* To whom correspondence should be addressed. Telephone: 852-2358-7352. Fax: 852-2358-1594. E-mail: chguo@ust.hk.

[1] Abbreviations: TEII, type II thioesterase; TE, thioesterase domain; DHB, dihydroxybenzoate or dihydroxybenzoyl; ArCP, aryl-carrier protein; PCP, peptidyl carrier protein; ACP, acyl carrier protein; A, adenylation domain; C, condensation domain; CoA, coenzyme A; 4-HBT, 4-hydroxybenzoyl-CoA thioesterase; IPTG, isopropyl β-D-thiogalactopyranoside; DCC, *N*,*N*′-dicyclohexylcarbodiimide; DTNB, 5,5′-dithio-bis(2-nitrobenzoic acid); NRPS, nonribosomal peptide synthetase; PBS, phosphate buffered saline; HPLC, high performance liquid chromatography; DTT, dithiothreitol; ATP, adenine 5′-triphosphate.

10.1021/bi802165x CCC: $40.75
Published on Web 02/04/2009

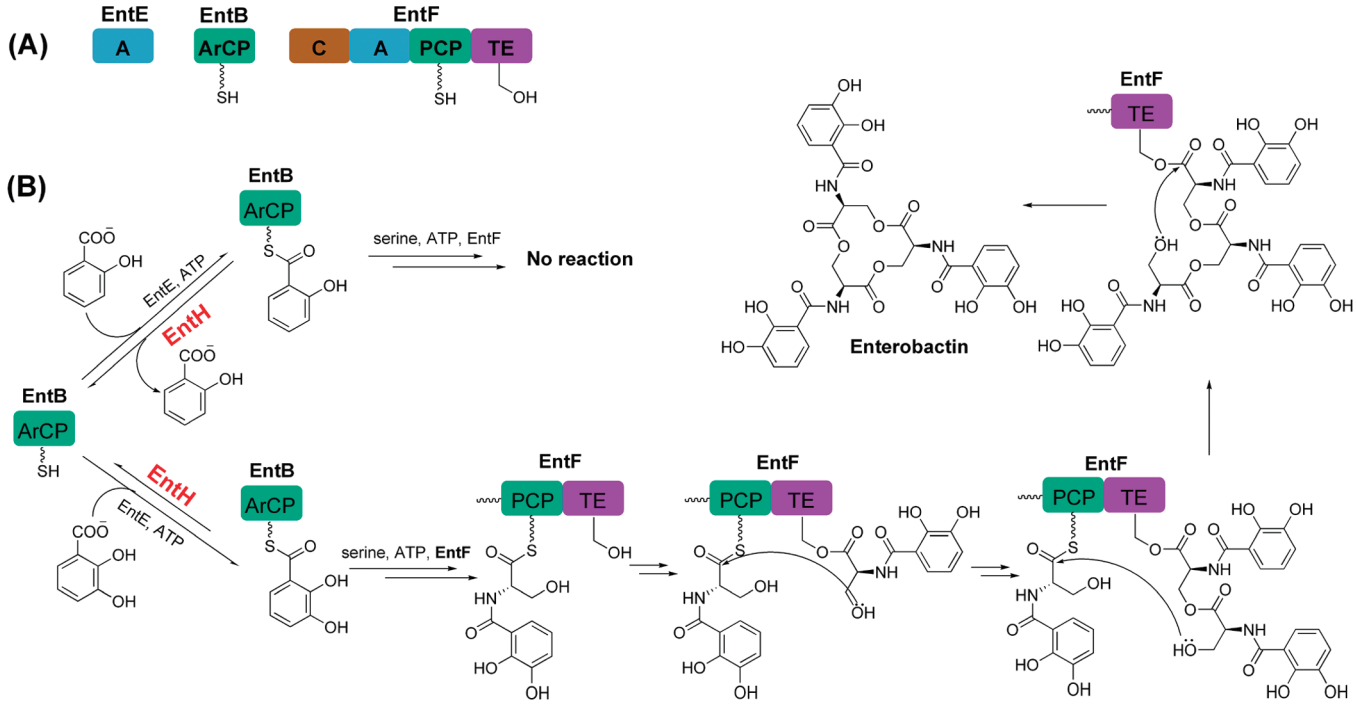

FIGURE 1: (A) Domain structure of the nonribosomal enterobactin synthase from *Escherichia coli*. (B) Biosynthesis of enterobactin and the proposed editing of misincorporated salicylyl precursor by the type II thioesterase EntH. The isochorismatase domain of EntB is omitted for simplicity. Key: A, adenylation domain; C, condensation domain; ArCP, aryl carrier protein; PCP, peptidyl carrier protein; TE, thioesterase domain (type I); vertical ~, phosphopantetheinyl tether.

whereas the first three domains of EntF activate serine and condense it with 2,3-DHB-ArCP to form a 2,3-DHB-seryl-PCP monomer, which is trimerized and cyclolactonized to form enterobactin by the terminal type I thioesterase domain (*18, 19*). Like other NRPSs, the enterobactin synthetase is also associated with a type II thioesterase EntH, or YbdB, or P15, which has recently been shown necessary for optimal production of the siderophore (*12*). Expression of EntH was found to restore enterobactin production that is significantly reduced in *entH*$^-$ mutants and in the presence of salicylate, which can be charged to the ArCP by EntE but cannot be processed by other functional domains of the enterobactin synthetase (*15*). This restoration ability of EntH was linked to its interaction with the ArCP domain of EntB and is consistent with a proofreading activity for the protein to remove wrongly charged precursor molecules on the ArCP (*12*).

EntH (YbdB) has been crystallized (PDB code: 1VH9) and found to possess a six-stranded antiparallel β-sheet wrapped around an elongated α-helix, like a hotdog "bun" wrapping around a "sausage", which is a typical three-dimensional architecture of hotdog fold superfamily proteins (*20*). Since it was first observed in the structure of *E. coli* β-hydroxydecanoyl thioester dehydratase FabA (*21*), the hotdog fold has been found to encompass a large number of proteins involved in metabolism, gene regulation, and signal transduction (*22*). Thioesterases are a prominent group of proteins in the hotdog fold superfamily and have been intensely investigated for their diverse biological functions, evolution, and catalytic mechanism in relation to their crystallographic structures (*22*−*27*). A general feature of these thioesterases is that they have a low degree of amino acid sequence conservation despite the conserved hotdog fold. Another characteristic of the thioesterases is that they exhibit high activity toward a broad spectrum of substrates, indicative of low substrate specificity. Correspondingly, hotdog thioesterases lack a well conserved set of active-site residues. For example, both the 4-hydroxybenzoyl-CoA thioesterase from *Arthrobacter* sp. strain CBS-3 (*28*−*30*) and the 4-hydroxybenzoyl-CoA thioesterase from *Pseudomonas* sp. strain SU (*31, 32*) are hotdog fold proteins and exhibit equivalent catalytic efficiencies, substrate specificities, and metabolic functions. However, they demonstrate distinctive quaternary structures, coenzyme A binding sites, and catalytic platforms. Among the hotdog fold thioesterases, only one carboxylate residue, Asp or Glu, is generally found to serve as a catalytic base or nucleophile in a variety of structural contexts in the thioester hydrolysis (*22*). Due to this high flexibility of active-site structures, it is difficult to predict from either the amino acid sequence or the crystallographic structure how EntH carries out its proofreading activities in enterobactin biosynthesis.

EntH is the first hotdog protein that has been suggested to be involved in proofreading a nonribosomal biosynthesis pathway. In this study, we report direct evidence for its proofreading activity by its restoration of enterobactin synthesis blocked by 2,3-DHB analogs, its substrate specificities, and structural basis for its editing activity. These studies show that EntH is able to preferentially hydrolyze the aberrant aryl intermediates by a built-in mechanism, which may allow it to adopt a more active proofreading mechanism than previously suggested for other similar editing type II thioesterases.

MATERIALS AND METHODS

Materials and General Methods. L-Serine, adenosine 5′-triphosphate (ATP) and crowding agent Ficoll 70 were purchased from Sigma-Aldrich. Benzoic acid, salicylic acid, 3-hydroxybenzoic acid, 4-hydroxybenzoic acid, 2,3-dihy-

droxybenzoic acid, 2,4-dihydroxybenzoic acid, 3,4-dihydroxybenzoic acid, 3,5-dihydroxybenzoic acid, *N*-hydroxysuccinimide (NHS), *N*,*N*′-dicyclohexylcarbodiimide (DCC), *N*-aetylcysteamine, 5,5′-dithiobis(2-nitrobenzoic acid) (DTNB), coenzyme A sodium salt hydrate (CoA-SH), and palmitoyl coenzyme A lithium salt were also purchased from Sigma-Aldrich. DNA-manipulating biochemicals, including restriction enzymes, T4 DNA ligase, and associated reagents, were obtained from New England Biolabs. Quick Change Site-Directed Mutagenesis kits for mutants were purchased from Stratagene. Other chemicals and biochemicals were obtained from commercial sources with the highest possible quality and used directly without further treatment, unless stated otherwise. Polymerase chain reaction (PCR) amplifications were performed with a PTC-200 Peltier Thermal Cycler from MJ Research. Protein chromatography was performed on a Bio-Rad BioLogic HR Workstation in a refrigerated chamber. HPLC analysis and purification were carried out using a Waters 600E system with Model 2487 dual λ absorbance detector. UV−vis absorbance was measured using a Perkin-Elmer Lambda 900 UV/vis/NIR spectrometer. Determination of molecular weights by mass spectroscopy was carried out with an API Q-Star Pulsar I quadrupole time-of-flight mass spectrometer. Nuclear magnetic resonance (NMR) spectrums were taken on 400 or 300 MHz Bruker spectrometers. Structure alignment was obtained from an EBI Tool−DaliLite Pairwise comparison of protein structures.

Protein Overexpression and Purification. The enterobactin biosynthetic proteins including *apo*-EntB, EntD, EntE, *apo*-EntF, and the type II thioesterase EntH (YbdB or p15) were overexpressed and purified to homogeneity as described previously (*33*). *apo*-EntB and *apo*-EntF were phosphopantetheinylated by a previously reported procedure using pure EntD. As demonstrated before, both EntB and EntF were confirmed to be correctly modified by an increase of mass of 340 Da, which is equivalent to addition of a phosphopantetheinyl group, in a MALDI-TOF mass spectroscopic analysis. EntH was expressed with a C-terminal hexahistidine tag similar to a reported method (*34*). Briefly, the gene of *ent*H was amplified from the genomic DNA of *E. coli* K12 using Phusion High-Fidelity DNA Polymerase from Finnzymes using ACATGCCATGGGAATGATCTGGAAACGCCATTTAACGCTC and ACCGCTCGAGTCCCAAAACTGCCGTACCCAGCCGA as primers. The PCR product was then digested by restriction enzymes and inserted into the pET-28a(+) vector (Novagen) between *Nco*I and *Xho*I. The *ent*H gene was confirmed not to contain any spurious mutations by sequencing the full length of the cloned insert. The gene product was expressed in Luria broth containing 0.2 mM IPTG at 37 °C for 4 h. EntH was purified from the crude extract prepared from the harvested cells, first by metal chelating chromatography using a 5 mL HiTrap Chelating HP column (GE Healthcare) and then by gel filtration using a Sephacryl S-100 column (GE Healthcare). SDS-PAGE found the obtained tagged protein was purified to greater than 95%. All the purified proteins were quantified by a Coomassie Blue protein assay kit (Pierce) and stored in PBS buffer (pH 7.4) containing 10% glycerol at −20 °C until use.

Site-Directed Mutagenesis. Expression plasmids of EntH mutants were constructed using the primers listed in the Supporting Information (Table S1) and the Quick Change Site-Directed Mutagenesis kit (Stratagene). All the mutated genes were confirmed by full-length DNA sequencing. The recombinant mutants were expressed in BL21 (DE3) in Luria broth containing 0.2 mM IPTG at 37 °C for 4 h and purified to greater than 95% by a combination of metal chelating chromatography and gel filtration. The purified proteins were also quantified by a Coomassie Blue protein assay kit (Pierce) and stored in PBS buffer (pH 7.4) containing 10% glycerol at −20 °C until use.

Gel Filtration and Circular Dichroism Spectrometry. Gel filtration was carried out on an Amersham Biosciences AKTA FPLC system using a Superose 12 10/300 column (GE Healthcare) at a flow rate of 0.5 mL/min. Protein samples were dissolved in 50 mM Tris−HCl buffer (pH 7.5) in the presence of 50 mM NaCl, 1 mM dithiothreitol, and 1 mM EDTA. The column was calibrated with the low molecular mass column calibration kit from GE Healthcare. Circular dichroism experiments were performed on a JASCO J-810 spectropolarimeter at 23 °C. The enzyme samples (final concentration 20 μM) were prepared in a cuvette with a path length of 1 mm in PBS buffer (pH 7.4) containing 10% glycerol. Each spectrum was averaged from three independent scans at 0.1 nm intervals and smoothed with a program accompanying the instrument.

Enzyme Assays. The activity of the enterobactin synthetase and its inhibition by salicylate or other aberrant precursors was assayed with an HPLC-based method with minor modifications (*34*). Briefly, a typical reaction contained EntH and the inhibitor at appropriate concentrations, 1 μM EntE, 6 μM *holo*-EntB, 50 nM *holo*-EntF, 1.5 mM 2,3-DHB, 10 mM ATP, 1.5 mM L-serine in 75 mM Tris−HCl (pH 7.5) buffer supplemented with 10 mM $MgCl_2$, 5 mM DTT, and 30% (w/v) Ficoll 70. Aliquots (100 μL each) were taken from the reaction mixture at an appropriate time interval and quenched immediately by addition of 10 μL of 1 N HCl. The products formed in the reactions were then analyzed by the same reported assay using ethyl acetate extraction. The slope of the plot of enterobactin concentration vs time for the first 12 min of the reaction was taken as the initial reaction rate.

A reported method (*33*) was modified for the measurement of the EntH thioesterase activity toward coenzyme A or *N*-acetylcystamine (NAC) thioester substrates. The newly released free thiol was monitored in real time at 412 nm in the presence of excess Ellman's reagent (dithiobisnitrobenzoic acid, DTNB). Each assay reaction was carried out at 23 °C in a 150 μL mixture containing DTNB (1−4 mM), a thioester substrate (12.5−800 μM), EntH or its mutants, and 100 mM phosphate buffer (pH 8.0). The kinetic parameters V_{max} and K_M were determined from initial velocity data, measured as a function of substrate concentration, using the Michaelis−Menten equation. To assay the enzyme activity for the native aryl-ArCP substrates, *apo*-EntB was phosphopantetheinylated at 37 °C for 30 min in 1 mL solution (in 75 mM Tris−HCl, 10 mM $MgCl_2$, pH 7.5) containing 800 μM *apo*-EntB, 15 μM EntD, and 4 mM salicylyl-CoA (or 4 mM 2,3-DHB-CoA in order to prepare 2,3-DHB-ArCP). After aryl-CoA was removed by gel filtration, the post-translational modification of EntB was found to be complete by native-gel electrophoresis and used immediately for activity assay in 100 mM sodium phosphate buffer (pH 7.0). The hydrolytic rate was determined by monitoring the

absorbance difference between the hydrolytic product and the substrate thioester at 325 nm for salicylyl-ArCP ($\Delta\varepsilon$ = 3500 $M^{-1}cm^{-1}$) and at 345 nm for 2,3-DHB-ArCP ($\Delta\varepsilon$ = 1900 $M^{-1}cm^{-1}$).

To determine the pH rate profiles, the kinetic parameters k_{cat} and K_M were determined in 100 mM sodium phosphate buffer at varied pH by measuring the initial velocity at different substrate concentrations through real-time monitoring of the absorbance at 325 nm for salicylyl-CoA ($\Delta\varepsilon$ = 3500 M^{-1} cm^{-1} for pH 6.0−8.0; $\Delta\varepsilon$ = 3300 M^{-1} cm^{-1} for pH 5.5, 8.5, and 9.0; $\Delta\varepsilon$ = 2300 M^{-1} cm^{-1} for pH 5.0 and 9.5; and $\Delta\varepsilon$ = 1800 M^{-1} cm^{-1} for pH 10.0) and at 345 nm for 2,3-DHB-CoA ($\Delta\varepsilon$ = 1900 M^{-1} cm^{-1} for pH 6.5−8.0; $\Delta\varepsilon$ = 1800 M^{-1} cm^{-1} for pH 8.5; $\Delta\varepsilon$ = 1700 $M^{-1}cm^{-1}$ for pH 6.0 and 9.0; $\Delta\varepsilon$ = 1500 M^{-1} cm^{-1} for pH 5.5; $\Delta\varepsilon$ = 1400 M^{-1} cm^{-1} for pH 9.5; $\Delta\varepsilon$ = 800 M^{-1} cm^{-1} for pH 10.0; and $\Delta\varepsilon$ = 600 M^{-1} cm^{-1} for pH 5.0). The plots of $\log(k_{cat})$ and $\log(k_{cat}/K_M)$ vs pH were fitted using the following equation: $\log Y = \log\{C/(1 + [H^+]/K_a + K_b/[H^+]\}$ where Y is k_{cat} or k_{cat}/K_M, $[H^+]$ is the proton concentration, C is the pH independent value of k_{cat} or k_{cat}/K_M, K_a is the acid dissociation constant, and K_b is the base dissociation constant (*35*).

Synthesis of Thioester Substrates. Thioester substrates of EntH were prepared by activation of the carboxyl group with NHS and subsequent esterification with corresponding thiols similar to a reported synthetic strategy (*36*). A typical activation reaction contained 3 mmol of unprotected benzoic acid or its derivative and 6 mmol of NHS in 5 mL of THF, and 6 mmol of DCC in 5 mL of THF was added to the reaction under a positive nitrogen pressure. After being stirred for 5 h at room temperature, the reaction mixture was filtered and the filtrate applied to a silica gel column and purified by flash chromatography (eluted by ethyl acetate−hexane) to give pure NHS esters. In the synthesis of coenzyme A thioesters, a solution of 0.1 M NHS ester in 1 mL of THF was added to 1 mL of CoA-SH (0.026 mmol) in water under a positive nitrogen pressure and, after adjusted to pH 8.0 by adding 1 N NaOH, the resulting solution was allowed to react for 1 h under continuous agitation at room temperature. In the synthesis of the NAC thioester, the activated NHS ester (0.1 M in 1 mL of THF) was added to 0.1 M NAC-SH, adjusted to pH 8.0 by adding triethylamine, and agitated continuously for 2 h under a positive nitrogen pressure at room temperature. After the reactions, the organic solvent of the reaction mixture was evaporated under reduced pressure, and the residue was purified on an Xterra preparative C18 reverse-phase column (10 μm particle size, 19 × 150 mm) on a Waters 600 HPLC system and a linear gradient from (90% A + 10% B) to (50% A + 50% B) over 40 min at a flow rate of 8 mL/min. Solution A was a 50 mM aqueous solution of ammonium acetate at pH 5.9, and solution B was 100% methanol. The fractions containing the thioesters were pooled, concentrated under reduced pressure to remove methanol, and then lyophilized to obtain the product with a 31−79% yield. A total of eight aryl-CoA and two aryl-NAC thioesters were prepared. The Supporting Information provides the characterization data for the NHS-activated intermediates and the final products by nuclear magnetic resonance spectroscopy and mass spectrometry.

RESULTS

Reconstitution of Nonribosomal Enterobactin Synthesis and Its Inhibition by 2,3-DHB Analogs. In vitro reconstitution of the enterobactin synthetase from EntE, EntB, and EntF was first achieved by Walsh and co-workers using 2,3-DHB and serine as the precursors (*15*). It was found that salicylate, a 2,3-DHB analog lacking the 3-hydroxyl group, was efficiently activated by EntE and charged to the ArCP domain of EntB. However, replacement of 2,3-DHB by salicylate in the reconstitution failed to produce any product. This salicylate effect indicates that the salicylyl group blocks the nonribosomal assembly line and is consistent with the in vivo finding that salicylate feeding significantly reduces the production of enterobactin (*12*). To further investigate the inhibiting effect of salicylate and demonstrate the proofreading activity of EntH, the enterobactin synthetase was prepared from EntE, *holo*-EntB, and *holo*-EntF. The in vitro enterobactin synthesis was carried out in the presence of 30% Ficoll 70 to suppress the production of linear side products (*34*).

As shown in Figure 2A, enterobactin was produced by the synthetase from 2,3-DHB, serine, and ATP in the absence of 2,3-DHB analogs. However, the enterobactin production was greatly diminished in the presence of equimolar salicylate and was virtually negligible when the ratio of salicylate to 2,3-DHB concentration was more than 10 (data not shown). In the absence of 2,3-DHB analogs, the time curve of enterobactin synthesis is linear for the first hour and extends well beyond 2 h with a nonzero rate. In the presence of salicylate, the reaction rate slows down and eventually decreases to zero, leading to a plateau in the curve (Figure 2B). As the salicylate to 2,3-DHB ratio is increased, the plateau level is quickly decreased while the time needed to reach the plateau is greatly shortened. This inhibition kinetics is consistent with a model in which the ArCP with a 2,3-DHB analog cannot be processed to form a cyclic product like enterobactin and are accumulated over time to finally terminate all synthetic activities. Other 2,3-DHB analogs, including benzoate, 3-hydroxybenzoate, 4-hydroxybenzoate, 2,4-DHB, 3,4-DHB and 3,5-DHB, were also found to inhibit the enterobactin production with a varying extent (Figure 2A). These results show that many benzoic acid derivatives other than salicylate can also be wrongly incorporated into the enterobactin assembly line at the ArCP and block the siderophore production.

Restoration of Blocked Enterobactin Synthesis by EntH. EntH was then added to the reaction mixture to test its ability of restoring enterobactin synthesis in the presence of the 2,3-DHB analogs. The siderophore production in the presence of an equimolar salicylate was indeed recovered quickly in the presence of the thioesterase at a low concentration, reaching at about 10 nM a production level close to that in the absence of salicylate (Figure 2C). However, EntH at a concentration greater than 10 nM decreased the enterobactin production. This conclusion is supported by the EntH effects on the initial rate for the NRPS in the presence of salicylate. As shown in Figure 3, 10 nM EntH causes a small NRPS reaction rate decrease (∼15%) and keeps it from disruption by salicylate over a wide concentration range. When the EntH concentration is increased, the range of salicylate concentration over which it can protect the NRPS is actually narrowed while the reaction rate is steadily decreased. Noticeably, EntH

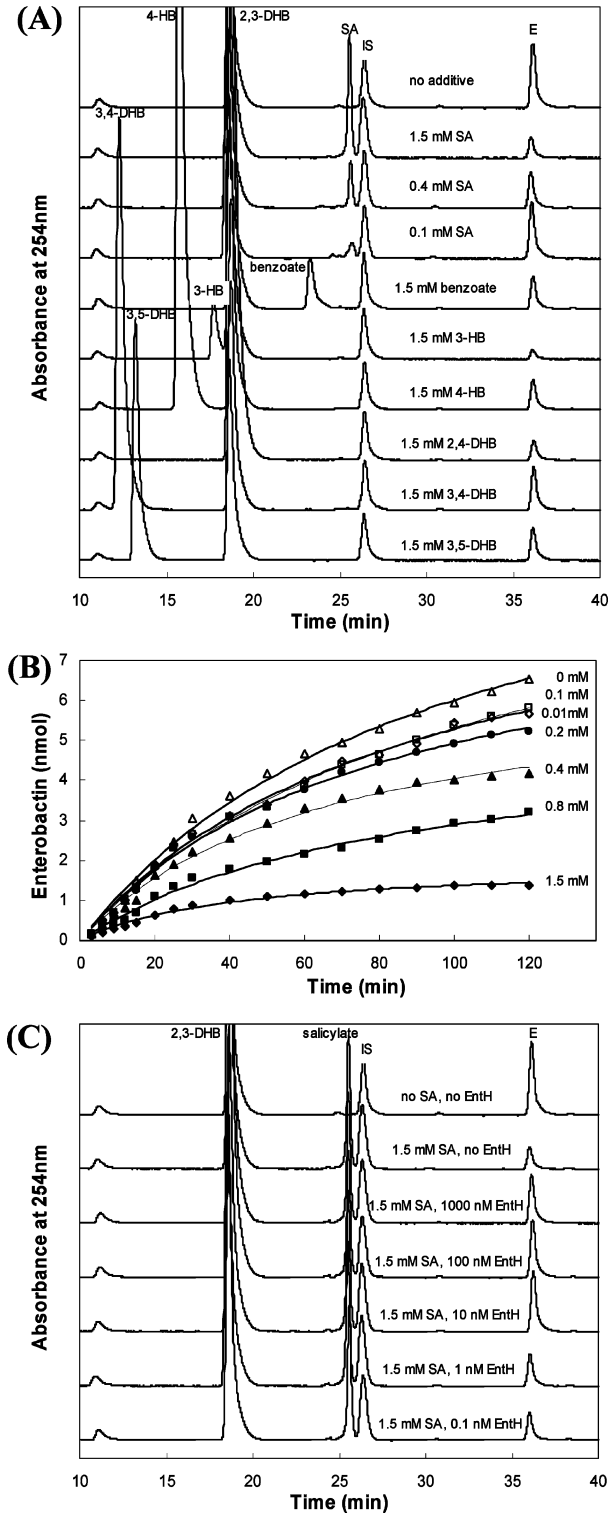

FIGURE 2: Inhibition of the reconstituted enterobactin synthetase by analogs of 2,3-dihydroxybenzoate, and restoration of enterobactin synthesis by EntH. (A) HPLC traces of the reconstituted in vitro enterobactin synthesis in the absence and presence of various 2,3-dihydroxybenzoate analogs. (B) Kinetics of the inhibition of enterobactin synthetase by salicylate. (C) Restoration of enterobactin synthesis by EntH in the presence of 1.5 mM salicylate. Besides EntH, a typical reaction contained 1 μM EntE, 6 μM *holo*-EntB, 50 nM *holo*-EntF, 1.5 mM 2,3-DHB, 10 mM ATP, 1.5 mM L-serine in 75 mM Tris−HCl (pH 7.5) buffer supplemented with 10 mM $MgCl_2$, 5 mM DTT, and 30% (w/v) Ficoll 70, and the reaction was quenched by HCl after 1.5 h at room temperature. SA, salicylate or salicylic acid; IS, internal standard = ethyl 3,4-dihydroxybenzoate; E, enterobactin; HB, hydroxybenzoic acid or hydroxybenzoate.

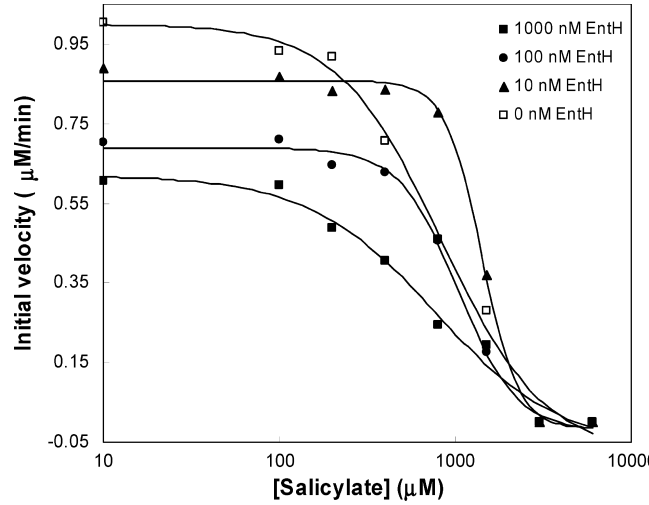

FIGURE 3: Change of the initial reaction rate of the enterobactin NRPS with the concentration of salicylate in the presence and absence of EntH. The concentration of the normal substrate, 2,3-dihydroxybenzoate, is 1.5 mM, and the reaction rate is expressed as the rate of formation of enterobactin.

at any concentration loses protective ability for the NRPS when 2,3-DHB is 1.5 mM and salicylate exceeds ~5.0 mM. Inhibition of the siderophore production by other 2,3-DHB analogs was also efficiently restored by 10 nM EntH (data not shown).

Substrate Specificities of EntH. Three groups of thioesters were used in an attempt to define the structural preference of EntH for its substrates. The first group includes two aryl-ArCP protein substrates that are the native substrates for EntH in its proofreading activity. The aryl group in the substrate is 2,3-dihydroxybenzoyl and salicylyl, respectively. Both substrates were prepared in situ from aryl-CoA in the presence of *apo*-EntB and EntD and used immediately in determination of kinetic parameters. The arylation of EntB was confirmed to be complete by native-gel electrophoresis. The second group substrate analogs are thioesters of 2,3-DHB and salicylate with *N*-acetylcysteamine (NAC), which has been generally used to mimic the phosphopantetheinyl linker of the carrier proteins in biochemical studies of polyketide and nonribosomal peptide synthetases. The third group substrate analogs are coenzyme A thioesters of various benzoate derivatives including 2,3-DHB and salicylate. Both the NAC and CoA thioesters were chemically synthesized and purified by HPLC.

Kinetic parameters of EntH were determined by measurement of initial velocities at various concentrations of the substrates or substrate analogs and are listed in Table 1. Interestingly, the TEII is able to distinguish the normal 2,3-DHB-ArCP substrate from the aberrant salicylyl-ArCP by exhibiting a 14.8-fold k_{cat}/K_M difference in favor of the latter. For corresponding coenzyme A thioesters, EntH exhibits comparable selectivity toward the substrate derived from the aberrant salicylate precursor while its kinetic parameters are hardly changed. In contrast, the corresponding NAC thioesters are not hydrolyzed by the TEII. These results show that EntH mainly recognize its substrates through interaction with the aryl group and the phosphopantetheinyl tether, but not the polypeptide moiety. They also indicate that the coenzyme A thioesters are good mimics of the native substrates and

Table 1: Steady-State Kinetic Parameters for Wild-Type EntH at Room Temperature

substrate	K_M (μM)	k_{cat} (s^{-1})	k_{cat}/K_M (M^{-1} s^{-1})	relative k_{cat}/K_M
salicylyl-EntB	272	4.83	1.78×10^4	7.67
2,3-DHB-EntB	116	1.40×10^{-1}	1.20×10^3	0.52
salicylyl-NAC			no activity	
2,3-DHB-NAC			no activity	
salicylyl-CoA	176 ± 7	4.63 ± 0.17	$(2.70 \pm 0.10) \times 10^4$	11.6
2,3-DHB-CoA	161 ± 5	$(3.72 \pm 0.05) \times 10^{-1}$	$(2.32 \pm 0.05) \times 10^3$	1
benzoyl-CoA	475 ± 26	13.9 ± 0.4	$(2.93 \pm 0.07) \times 10^4$	12.6
3-hydroxybenzoyl-CoA	265 ± 8	10.3 ± 0.2	$(3.90 \pm 0.05) \times 10^4$	16.8
4-hydroxybenzoyl-CoA	190 ± 9	$(2.07 \pm 0.03) \times 10^{-1}$	$(1.09 \pm 0.22) \times 10^3$	0.47
2,4-DHB-CoA	219 ± 8	$(3.42 \pm 0.08) \times 10^{-2}$	$(1.55 \pm 0.02) \times 10^2$	0.067
3,5-DHB-CoA	256 ± 4	7.45 ± 0.08	$(2.90 \pm 0.02) \times 10^4$	12.5
3,4-DHB-CoA	212 ± 4	$(2.30 \pm 0.02) \times 10^{-1}$	$(1.08 \pm 0.01) \times 10^3$	0.47
palmitoyl-CoA	4.25 ± 0.06	$(1.54 \pm 0.01) \times 10^{-1}$	$(3.62 \pm 0.03) \times 10^4$	15.6
acetyl-CoA			no activity	

suitable for determination of the EntH specificities for the aryl moiety of the substrate.

Like other hotdog fold thioestereases, EntH is active toward a wide range of substrates including acyl-CoAs and aryl-CoAs. Its catalytic efficiency is generally 1−2 orders of magnitude lower than other hotdog fold proteins such as 4-HBT (*28*−*32*) or PaaI (*23*) but is significantly higher than the cellulose binding protein-fused EntH (*12*). EntH is unable to recognize short-chain acyl-CoAs, such as acetyl-CoA, but readily uses long-chain acyl-CoAs, such as palmitoyl-CoA, as a substrate. The Michaelis constants for aryl-CoA substrates are >50-fold higher than that for palmitoyl-CoA, but the turnover rate (k_{cat}) is much higher for some aryl-CoA substrates. Noticeably, EntH activity is sensitive to the pattern of hydroxyl substituents on the aryl-CoA substrates. Its Michaelis constant for the aryl-CoA substrates varies within a narrow 2-fold range, whereas the turnover rate (k_{cat}) varies widely in the range from 0.034 to 13.9 s^{-1} (409-fold difference). The catalytic efficiency of the TEII is highest when aryl-CoA contains no hydroxyl substituent or with one hydroxyl group at either an ortho- or a meta-position on the aromatic ring, while it is the lowest when there is a *para*-OH. Interestingly, the enzyme exhibits close to the lowest activity toward the substrate with OH groups at both ortho- and meta-positions, 2,3-DHB-CoA, which is derived from the native 2,3-DHB precursor for enterobactin biosynthesis.

Contribution of Substitution Effects to EntH Substrate Specificities. The phenolic hydroxyl groups of the EntH aryl-CoA substrates are capable of affecting the rate of the hydrolytic reactions through the electronic substitution effect. To understand the significance of this substitution effect in the enzymatic catalysis, the nonenzymatic hydrolytic rates of the coenzyme A thioester substrates were determined in the absence of the enzyme to find a reactivity order that is different from that for the EntH-catalyzed reaction. Comparing 3-hydroxylbenzoyl-CoA with 2,3-DHB-CoA for example, the nonenzymatic hydrolysis is 50% faster for the former when the reaction is affected only by the electronic substitution effect (Figure 4B), but the enzymatic hydrolysis is 16.8-fold faster for the latter substrate (Figure 4A). This difference indicates that the electronic substitution effect plays a limited role in the EntH specificities toward the pattern of phenolic hydroxyl groups in the substrates. It is noteworthy that EntH exhibits a Michaelis constant within a small 2-fold range for different benzoyl-CoA derivatives but has a widely varied turnover rate determines the relative catalytic efficiency (Table 1). The kinetic results for both the nonenzymatic and enzymatic reactions show that EntH achieves the unique substrate specificities mainly through differential stabilization or destabilization of the transition state in the enzymatic hydrolysis of different aryl substrates.

Quaternary Structure and pH Rate Profiles of EntH. The homogeneous EntH was a single symmetric peak in analytical gel filtration and was determined to have a molecular

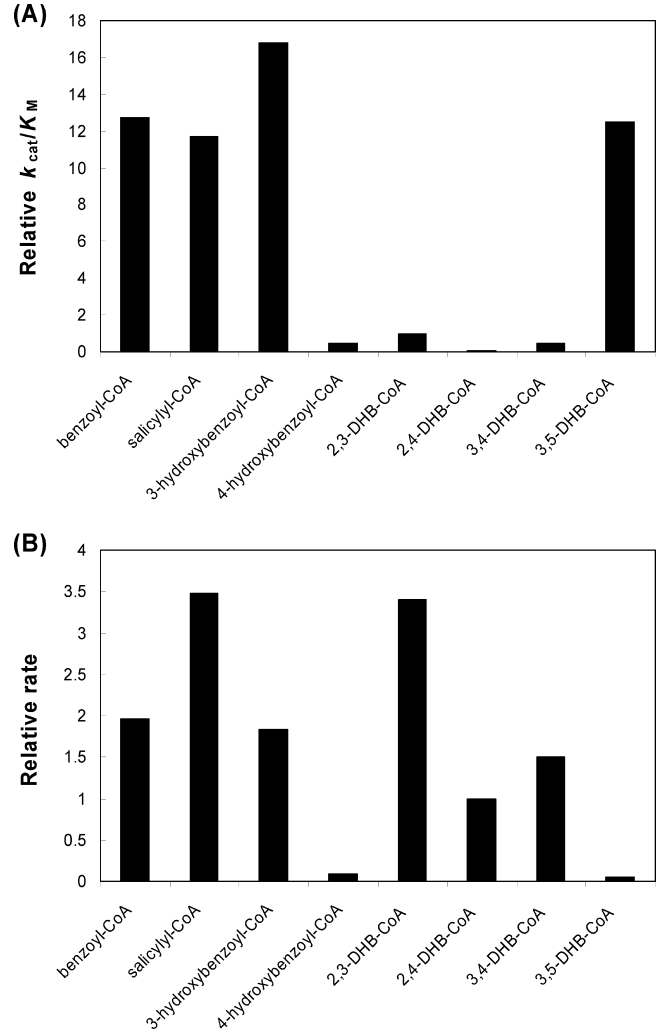

FIGURE 4: Relative hydrolytic rates of various aryl-CoA thioesters in the presence (A) and absence (B) of the type II thioesterase EntH. The relative EntH k_{cat}/K_M is normalized by setting the second-ordered enzymatic rate constant for 2,3-DHB-CoA to 1, while the relative pseudo-first-order rate constant of the spontaneous hydrolysis of a thioester in 100 mM phosphate buffer (pH 8.0) is calculated by setting the rate constant for 2,4-DHB-CoA to 1.

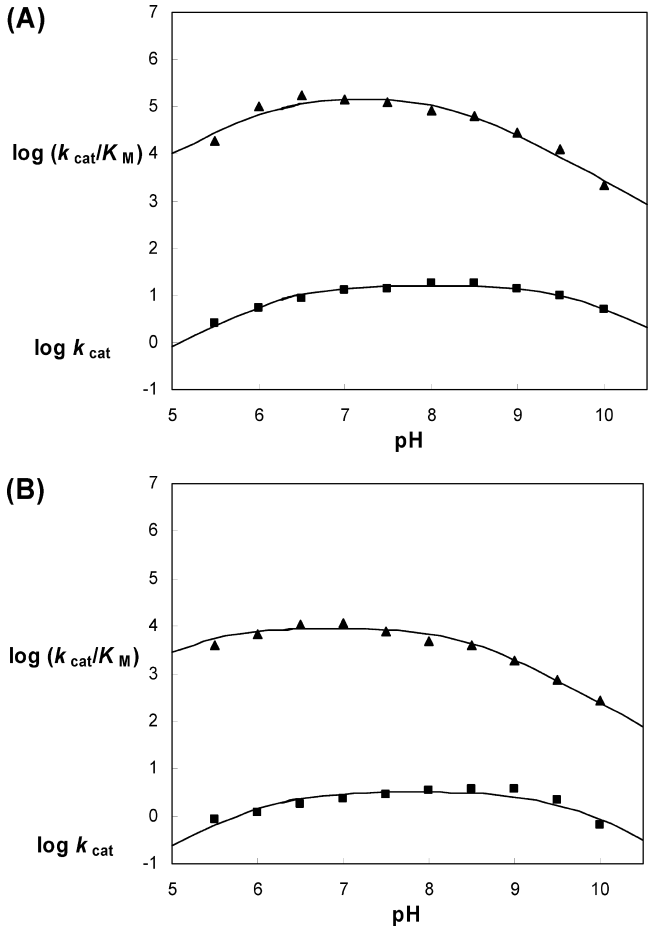

FIGURE 5: pH rate profiles of hydrolysis of salicylyl-CoA (A) and 2,3-DHB-CoA (B) catalyzed by EntH. The solid lines are fitting curves obtained from the equation log $Y = \log\{C/(1 + [H^+]/K_a + K_b/[H^+]\}$ where Y is k_{cat} or k_{cat}/K_M. Key: ▲, log (k_{cat}/K_M); ■, log (k_{cat}).

weight of 54.4 kDa. In comparison to the calculated monomeric size of 15.0 kDa, native EntH is a homotetramer. There is no unusual ultraviolet−visible absorption peak other than those typical of bovine serum albumin, indicating that the protein does not contain tightly bound coenzyme A like YciA (*27*), another hotdog thioesterase in *E. coli*.

The pH rate profiles of the EntH-catalyzed salicylyl-CoA and 2,3-DHB-CoA hydrolysis were determined as shown in Figure 5. They all conform to a simple model in which the enzymatic reaction relies on ionization of an essential base at low pH and on ionization of an essential acid at high pH (*35*). The bell-shaped curves were fitted to define the apparent pK_a values for ionization of essential residues in the enzyme−substrate complex (log(k_{cat})) and in the free enzyme (log(k_{cat}/K_M)). For the salicylyl-CoA hydrolysis, the log(k_{cat}) profile defines a pK_a of 6.3 ± 0.1 for ionization of an essential base, and an apparent pK_a of 9.6 ± 0.1 for ionization of an essential acid in the enzyme−substrate complex, whereas in the uncomplexed enzyme the log(k_{cat}/K_M) profile defines that the pK_a values for ionization of an essential base and an essential acid are 6.2 ± 0.2 and 8.2 ± 0.1, respectively. The pK_a values for the 2,3-DHB-CoA hydrolysis were 6.1 ± 0.2 and 9.5 ± 0.2, respectively, for the ionization of the essential base and the essential acid in the enzyme−substrate complex, and 5.4 ± 0.2 and 8.4 ± 0.1, respectively, for the essential base and essential acid ionization in the free enzyme. Coincidentally, pK_a of the salicylyl-CoA phenolic group, determined to be 9.4 by pH titration as monitored at 370 nm, is the same as the pK_a of the essential acid in the EntH-salicylyl-CoA complex. In the meantime, the pK_a for ionization of the 2,3-DHB-CoA phenolic hydroxyl groups is 8.7 (monitored at 380 nm), and 0.8 unit lower than the pK_a of the essential acid obtained from the log(k_{cat}) profile. These results indicate that the salicylyl-CoA phenolic hydroxyl group may be the essential acid contributing to the log(k_{cat}) profile and that the pK_a of the 2,3-DHB-CoA phenolic hydroxyl groups is dramatically changed upon binding to the enzyme active site, suggesting that the two substrates interact differently with the TEII.

Table 2: Structural Comparison between EntH and Other Hotdog Fold Proteins Using DaliLite

protein	PDB code	Z-score	aligned residues	rmsd (Å)	seq identity (%)
FcbC1[a]	1Q4T	19.0	128	1.8	30
HBT_PSEUC[b]	1LO7	10.0	102	2.4	8
FabA	1MKA	12.1	128	3.0	13
PaaI	1P5U	1.4	69	3.4	7
TesB	1C8U	13.8	106	2.4	8
YbaW	1NJK	9.8	99	2.2	11
YbgC	1S5U	11.2	101	2.1	6
YdiI	1VH5	26.9	138	0.5	59
YciA	1YLI	10.8	101	1.8	16

[a] FcbC1: 4-hydroxybenzoyl CoA thioesterase from *Arthrobacter* sp. strain SU. [b] 4HBT_PSEUC: 4-hydroxybenzoyl CoA thioesterase from *Pseudomonas* sp. strain CBS-3.

Structural Comparison of EntH with Other Hotdog Proteins. The EntH crystallographic structure (PDB code: 1VH9) is consistent with the EntH tetrameric quaternary structure determined in solution by gel filtration. It is similar to other tetrameric hotdog thioesterases containing the same number of β-sheet strands, such as 4-hydroxybenzoyl-CoA thioesterases (4-HBT) in the 4-chlorobenzoate dehalogenation pathway (*28, 30*), phenylacetyl-CoA thioesterase PaaI in the phenylacetate pathway (*23*), and *E. coli* medium chain length acyl-CoA thioesterase II (TesB) (*37*). Structural search using the DaliLite program (*38*) found that EntH is most closely similar to YdiI (Table 2), an *E. coli* hotdog protein without a known function. The closest EntH structural homologue with a known function is the 4-HBT from *Arthrobacter* sp. strain SU (*30*). Ignoring the short N-terminal α-helices, the remaining majority of the EntH structure almost completely superimposes on the *Arthrobacter* 4-HBT using the program Pymol (*39*) (Figure 6). Despite this high degree of structural resemblance, the two proteins share only 30% identity in their amino acid sequence.

The active site of the *Arthrobacter* 4-HBT has been defined by crystallographic studies of its complexes with its inhibitor, 4-hydroxyphenacyl-CoA, and its products, 4-hydroxybenzoate and coenzyme A (*30*). It is primarily wedged between the major α-helices in the two subunits comprising the dimer, containing Glu-73 from subunit II as a catalytic residue as supported by a 67 000-fold reduction in k_{cat} for its mutation to alanine and Gly-65 from subunit I whose peptidic NH polarizes the thioester C═O through hydrogen bonding for nucleophilic attack in the hydrolysis. Other active-site residues surrounding the 4-hydroxyphenacyl moiety include Met-74, Thr-77, Glu-78, and Gly-93 of the subunit II and His-64 and Gln-58 of the subunit I. In the superimposed structures (Figure 6C), the EntH residues corresponding to Glu-73 and Gly-65 of the *Arthrobacter*

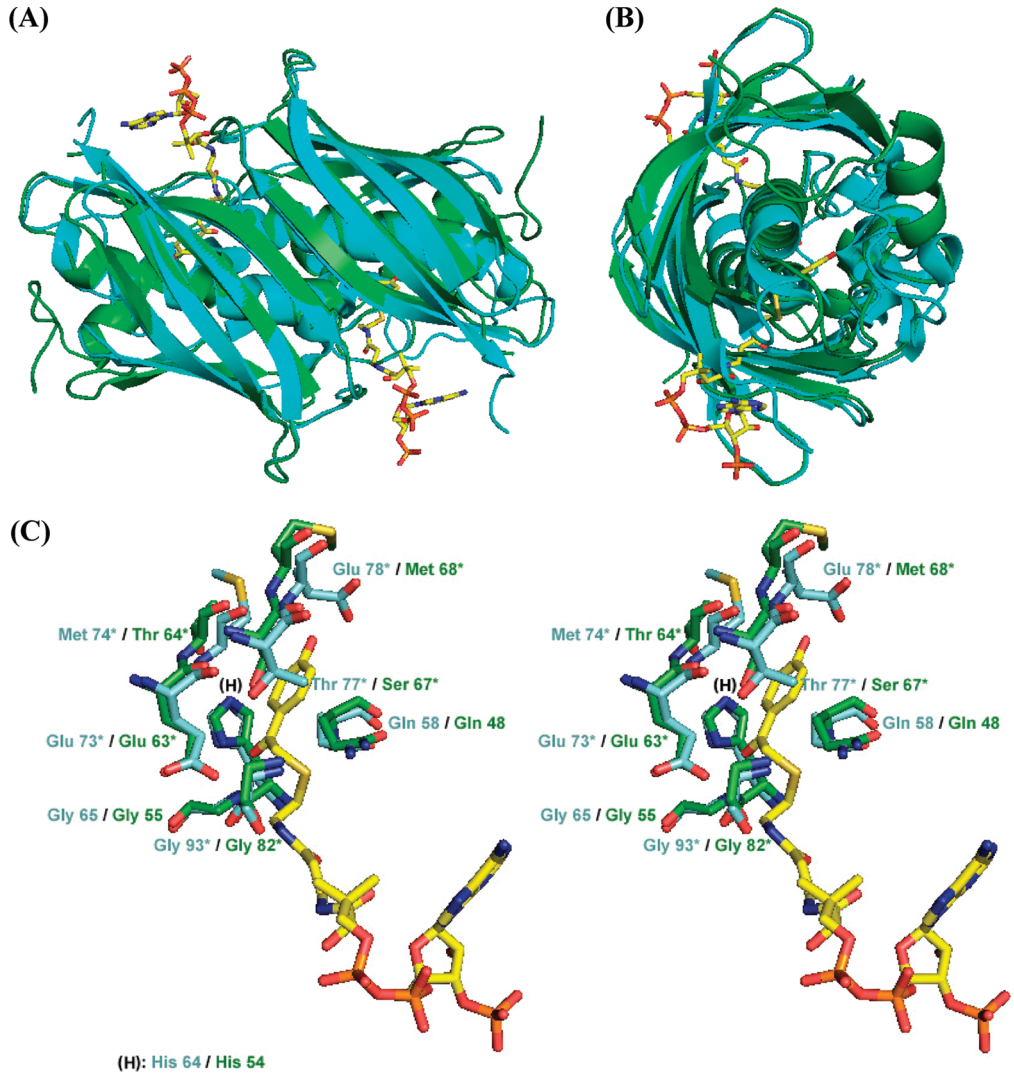

FIGURE 6: Superposition of the crystallographic structures of *E. coli* EntH (green) and *Arthrobacter* 4-hydroxybenzoyl-CoA thioesterase (blue) in complex with 4-hydroxyphenacyl-CoA inhibitor (yellow). (A) Ribbon representation of the overlaid structures. (B) View of the overlaid structures rotated 90° along the dyad axis. (C) Stereoview of the region corresponding to the active site of the *Arthrobacter* 4-hydroxybenzoyl-CoA thioesterase in the superimposed structures. The figures were generated from the *E. coli* EntH (PDB code: 1VH9) and the 4-hydroxybenzoyl-CoA thioesterase from *Arthrobacter* sp. Strain SU (PDB code: 1Q4T) in complex with 4-hydroxyphenacyl-CoA using the program Pymol. The active-site residues are represented by ball-and-stick drawings, and the residues belonging to the second subunit of the dimer are marked by an *.

4-HBT are Glu-63 of subunit II and Gly-55 of subunit I, respectively. Other EntH residues corresponding to the 4-hydroxyphenacyl group surrounding 4-HBT residues are Thr-64, Ser-67, Met-68, and Gly-82 of subunit II and His-54 and Gln-48 of subunit I. EntH contains no amino acid residues corresponding to Ser-120 and Thr-121 from subunit III of the *Arthrobacter* 4-HBT tetramer, which form hydrogen bonds with the pyrophosphate moiety of the coenzyme A product (*31*). Due to the high degree of structural overlap between the two enzymes, the EntH active site is believed to consist of Gln-48, Gly-55, Glu-63, Thr-64, Ser-67, Met-68, and Gly-82.

Steady-State Kinetics of the Active-Site Mutants. The suspected active-site residues were individually replaced by alanine or other amino acid residues to test their contribution to the hydrolytic catalysis. All these site-directed mutants were overproduced equally well as the wild-type EntH and found to present a far UV circular dichroism spectrum that overlaps that of the wild-type protein (data not shown), indicating that the EntH conformation is minimally affected by the point mutations. Table 3 summarizes the results of steady-state kinetic characterization of these mutants toward a good substrate, salicylyl-CoA. No catalytic activity was found for Q48A and all mutants at Glu-63, whereas a 290-fold decrease of catalytic efficiency was found for the Q48N mutant. In the meantime, mutation of other identified amino acid residues also leads to significant activity loss. The decrease in catalytic efficiency is 13-fold for T64S, 140-fold for S67A, 130-fold for M68A, and 229-fold for H54A. These kinetic parameters of the mutant enzymes strongly support that the amino acid residues identified in the structural comparison are indeed the active-site residues of the thioesterase EntH.

The site-directed mutants were also kinetically characterized for 2,3-DHB-CoA (Table 3), the analog of the normal precursor on the ArCP of the enterobactin NRPS. In comparison to the kinetic parameters for salicylyl-CoA, the analog of the aberrant precursor on the enterobactin assembly line, most mutant enzymes exhibit higher activities toward the aberrant intermediate like the wild-type enzyme. How-

Table 3: Steady-State Kinetic Parameters for Wild-Type EntH and Its Mutants at Room Temperature

	salicylyl-CoA			2,3-dihydroxybenzoyl-CoA			relative
variant	K_M (μM)	k_{cat} (s^{-1})	k_{cat}/K_M (M^{-1} s^{-1})	K_M (μM)	k_{cat} (s^{-1})	k_{cat}/K_M (M^{-1} s^{-1})	k_{cat}/K_M
wild type	176 ± 7	4.63 ± 0.17	$(2.70 \pm 0.10) \times 10^4$	161 ± 5	$(3.72 \pm 0.05) \times 10^{-1}$	$(2.32 \pm 0.05) \times 10^3$	11.6
E63A				no activity			
E63D				no activity			
E63Q				no activity			
Q48A				no activity			
Q48N	729 ± 19	$(6.78 \pm 0.27) \times 10^{-2}$	$(9.30 \pm 0.2) \times 10^1$	505 ± 55	$(1.55 \pm 0.10) \times 10^{-2}$	$(3.10 \pm 0.43) \times 10^1$	3.0
H54A	162 ± 12	$(1.90 \pm 0.05) \times 10^{-2}$	$(1.18 \pm 0.06) \times 10^2$	37.5 ± 6.8	$(2.17 \pm 0.17) \times 10^{-3}$	$(5.83 \pm 0.87) \times 10^1$	2.02
T64S	672 ± 50	1.38 ± 0.04	$(2.07 \pm 0.10) \times 10^3$	383 ± 39	$(1.38 \pm 0.03) \times 10^{-1}$	$(3.60 \pm 0.30) \times 10^2$	5.75
S67A	263 ± 23	$(5.07 \pm 0.22) \times 10^{-2}$	$(1.93 \pm 0.10) \times 10^2$	329 ± 32	$(1.12 \pm 0.10) \times 10^{-2}$	$(3.42 \pm 0.17) \times 10^1$	5.64
S67C	196 ± 1	$(5.10 \pm 0.03) \times 10^{-2}$	$(2.60 \pm 0.02) \times 10^2$	454 ± 70	$(3.33 \pm 0.33) \times 10^{-3}$	7.43 ± 0.01	35.0
M68A	373 ± 12	$(7.78 \pm 0.08) \times 10^{-2}$	$(2.08 \pm 0.03) \times 10^2$	1420 ± 160	$(5.33 \pm 0.32) \times 10^{-1}$	$(3.77 \pm 0.10) \times 10^2$	0.55

ever, the ability to selectively hydrolyze the aberrant intermediate, as represented by the relative k_{cat}/K_M, is reversed for the M68A mutant and significantly decreased for most other mutants, of which H54A has the lowest selectivity (Table 3). These results indicate that the active-site residues, including Thr-64, Ser-67, His-54, and Met-68, all contribute to the distinction between the normal and aberrant intermediates by the thioesterase with the most contribution coming from the last two amino acid residues.

DISCUSSION

In this study, we have demonstrated disruption of the nonribosomal enterobactin synthesis by aberrant precursors and restoration of the disrupted enterobactin synthesis by the proofreading thioesterase EntH. This is the first demonstration of editing activities of a TEII in a fully reconstituted NRPS system. Results from these restoration experiments are fully consistent with the in vivo observations that only a low level of EntH is required to restore the enterobactin synthesis blocked by the aberrant precursors, and that expression of EntH at a high level is actually detrimental to the yield of the siderophore (*12*). They provide direct supporting evidence for the suggested role of EntH to hydrolyze the aberrant aryl-ArCP as well as the normal 2,3-DHB-ArCP (*12*).

The physiological role of EntH as a proofreading enzyme is closely related to its substrate specificities. The TEII is inactive toward short-chain acyl thioesters and is thus unable to hydrolyze misacylated ArCP or PCP, which has been suggested to be the physiological substrate of editing TEIIs (*7*). This activity deficiency indicates that EntH is not responsible for regeneration of misprimed enterobactin synthase, which may be accomplished by yet another undiscovered TEII. Alternatively, mispriming may be negligible due to more stringent substrate specificities of the 4-phosphopantetheinyltransferase EntD. Currently, it is not known whether EntD is able to prevent misacylation of ArCP or PCP by rejecting short-chain acyl-CoA as substrate. On the other hand, EntH exhibits high catalytic activity toward aryl thioesters and is able to recognize the benzene ring hydroxylation pattern on its aryl-ArCP substrates. In comparison to the thioesters of the normal 2,3-DHB precursor, EntH is at least 10-fold more efficient for the aryl thioesters derived from aberrant precursors with a hydroxylation pattern different from 2,3-DHB but without a *para*-OH. As a ubiquitous phytohormone in plant defense (*40*), salicylic acid is most abundantly present in the environment among these aberrant precursors, suggesting that the TEII might have been evolved to eliminate its disruption in enterobactin biosynthesis. However, the TEII demonstrates a low activity toward the thioester of another potential blocker of the nonribosomal synthesis, 4-hydroxylbenzoate of the ubiquinone biosynthetic pathway (*41*). Since this low activity has no observable effect on EntH ability in restoring enterobactin synthesis in vivo (*12*), the physiological concentration of this endogenous metabolite may be too low to cause serious disruption. Indeed, a micromolar level of 4-hydroxybenzoate is sufficient to sustain optimal growth of *Escherichia coli* (*42*).

The close resemblance of the active-site structures of EntH and *Arthrobacter* 4-HBT suggests similarities in their catalytic mechanism. Indeed, the absolute requirement of Glu-63 for the EntH hydrolytic activities strongly supports that this acidic residue serves as either the catalytic base or a catalytic nucleophile like its corresponding residue in the *Arthrobacter* 4-HBT, Glu-73 (*31*). This catalytic role of Glu-63 is also supported by the pH profile that indicates a catalytic base with a pK_a of 6.1−6.3 for its ionization, which is consistent with the acidity of the side-chain carboxylic acid. In addition, mutation of Gln-48 to alanine also leads to complete loss of the EntH activities, indicating that it significantly contributes to the enzyme catalysis like its corresponding Gln-58 in the *Arthrobacter* 4-HBT. Besides the Glu/Gln pairs in these two enzymes, a similar Asp-61/Asn-46 pair has been found to play similar essential roles in the catalysis of phenylacetyl-CoA thioesterase PaaI in the phenylacetate pathway (*23*), suggesting that the (Glu or Asp)/(Gln or Asn) pair is an important catalytic motif in hotdog fold thioesterases. Moreover, the structural superposition (Figure 6) showed that the EntH Gly-55 is equivalent to the *Arthrobacter* 4-HBT Gly-65, whose amide NH has been found to activate the thioester carbonyl by forming a hydrogen bond (*31*) and to likely stabilize the tetrahedral oxyanion intermediate in the catalyzed hydrolysis through hydrogen-bonding. Conservation of this glycine residue indicates that EntH is mechanistically similar to *Arthrobacter* 4-HBT by adopting the same mechanism for substrate activation and oxyanion stabilization.

Despite the similarities in three-dimensional structure and reaction mechanism, the *Arthrobacter* 4-HBT and EntH are subtly different in both substrate specificities and active-site configuration. Although both enzymes utilizes aryl thioesters as substrate and exhibit a broad substrate spectrum, the 4-HBT demonstrates the highest activity toward 4-hydroxybenzoyl-CoA, which is the poorest EntH substrate among the tested aryl-CoA substrates. This difference may be due to the substitution of the 4-HBT Glu-78, which may interact

favorably with the *para*-OH of the bound 4-hydroxylphenacyl-CoA, by Met-68 in the EntH structure, which is much more hydrophobic and repulsive to the polar *para*-OH. This expected discrepancy in substrate−enzyme interaction is supported by the higher affinity of 4-hydroxybenzoyl-CoA for 4-HBT than for EntH as indicated by their Michaelis constants at 1.2 (*32*) and 190 μM (Table 1), respectively. In addition, EntH demonstrates exquisite specificities to the benzene ring hydroxylation pattern on the aryl thioesters, which is crucial to its proofreading activity, whereas no similar hydroxylation sensitivity has been known for the 4-HBT.

One distinctive feature of the EntH active site is a strong hydrogen bond between the Thr-64 side chain hydroxyl and His-54 as indicated by a short distance of 2.9 Å between Thr-64 O^{γ} and Nε2 of the His-54 imidozole ring. In the 4-HBT active site, Met-74 from Subunit I/II occupies the equivalent position of EntH Thr-64 with an unknown impact on the enzyme activity. The Nδ1 of the His-54 side chain in EntH is 3.1 Å from the carbonyl oxygen of the 4-hydroxyphenacyl-CoA inhibitor in the superimposed structure (Figure 6C) but is unlikely to form a hydrogen bond with the latter because the $N_{\delta 1}\cdots O$ is almost perpendicular to the $N_{\delta 1}$-H bond. Thus, the $N_{\delta 1}$-H in the EntH His-54 side chain appears to be suitable to serve as a general acid to protonate the tetrahedral oxyanion resulting from the nucleophilic attack on the substrate carbonyl group, while the hydrogen bond between Thr-64 and His-54 serves to orient the imidazole ring of the latter residue to facilitate this proposed role. Consistently, mutation of His-54 leads to a 229-fold decrease in catalytic activity in which an active-site water may serve the role of a general acid in the absence of the imidazole ring.

In the absence of atomic details of substrate−EntH interaction, it is a challenge to understand the exquisite specificities of the thioesterase for the benzene ring hydroxylation patterns of the aryl thioester substrates. Consistent with the mutational results indicating that both His-54 and Met-68 play critical roles in the distinction between thioesters of the normal and aberrant precursors, side chains of these two residues are in close contact with the 4-hydroxyphenacyl-CoA inhibitor bound to the *Arthrobacter* 4-HBT in the superimposed structure with EntH (Figure 6). One possible explanation for EntH differentiation of substrates with or without only one hydroxyl group at either the ortho- or meta-position from the substrates with two hydroxyl groups at both of the positions (2,3-DHB-CoA or 2,3-DHB-ArCP) is that these substrates interact differently with side chains of both His-54 and Met-68 so that the coplanarity of the substrate phenyl ring with the carbonyl group undergoing nucleophilic attack results in different stabilization of the transition state and, consequently, the observed significant difference in the turnover rate (Table 1). Alternatively, the differential interaction between the substrates and the side chains may dislodge the His-54 imidazole ring to affect its likely role as a general acid and result in the detected k_{cat} difference. The difference in interaction of salicylyl-CoA and 2,3-DHB-CoA with EntH as suggested by the pH rate profiling (Figure 5) is supportive of the proposed differential interaction of the bound substrates with the active site. However, the details of these differential enzyme−substrate interactions are beyond comprehension at present and require further structural studies to clarify. Nonetheless, the distinctive EntH substrate specificities in relation to its active-site structure once again demonstrate the versatility of the catalytic platform of hotdog fold proteins, which allows fine-tuning of the constituent amino acid residues to meet different functional needs.

In summary, we have shown that the versatile hotdog fold structure allows the type II thioesterase EntH to achieve significantly higher catalytic efficiency toward the aberrant salicylyl precursor wrongly incorporated into the ArCP of the enterobactin assembly line. This EntH ability to distinguish between aberrant and normal intermediates suggests that the proofreading enzyme may be able to actively search for the aberrant intermediate for early elimination, rather than recognizing the aberrant intermediate through a passive kinetic control mechanism (*8*). Although the preferential removal of aberrant precursors has not been demonstrated for the few NRPS-type II thioesterases previously characterized (*7, 8*), a recent NMR study found that the TEII of surfactin NRPS shows high specificity for the acetyl group misprimed to the phosphopantotetheinyl group of PCP domains by having a small binding pocket (*43*). This recent development suggests that the preferential aberrant precursor removal by EntH is not an exception but, rather likely, a general feature of type II thioesterases in nonribosomal peptide synthesis.

SUPPORTING INFORMATION AVAILABLE

Primer sequences, preparation procedures, and characterization data for the *N*-hydroxysuccinimide esters, coenzyme A thioesters, and *N*-acetylcysteamine thioesters. This material is available free of charge via the Internet at http://pubs.acs.org.

REFERENCES

1. von Döhren, H., Keller, U., Vater, J., and Zocher, R. (1997) Multifunctional peptide synthetases. *Chem. Rev. 97*, 2675–2705.
2. Marahiel, M. A., Stachelhaus, T., and Mootz, H. D. (1997) Modular peptide synthetases involved in nonribosomal peptide synthesis. *Chem. Rev. 97*, 2651–2673.
3. Finking, R., and Marahiel, M. A. (2004) Biosynthesis of nonribosomal peptides. *Annu. Rev. Microbiol. 58*, 453–488.
4. Fischbach, M. A., and Walsh, C. T. (2006) Assembly-line enzymology for polyketide and nonribosomal peptide antibiotics: logic, machinery, and mechanisms. *Chem. Rev. 106*, 3468–3496.
5. Kohli, R. M., and Walsh, C. T. (2003) Enzymology of acyl chain macrocyclization in natural product biosynthesis. *Chem. Commun.* 297–307.
6. Kopp, F., and Marahiel, M. A. (2007) Macrocyclization strategies in polyketide and nonribosomal peptide biosynthesis. *Nat. Prod. Rep. 24*, 735–749.
7. Schwarzer, D., Mootz, H. D., Linne, U., and Marahiel, M. A. (2002) Regeneration of misprimed nonribosomal peptide synthetases by type II thioesterases. *Proc. Natl. Acad. Sci. U.S.A. 99*, 14083–14088.
8. Yeh, E., Kohli, R. M., Bruner, S. D., and Walsh, C. T. (2004) Type II thioesterase restores activity of a NRPS module stalled with an aminoacyl-S-enzyme that cannot be elongated. *ChemBioChem 5*, 1290–1293.
9. Schneider, A., and Marahiel, M. A. (1998) Genetic evidence for a role of thioesterase domains, integrated in or associated with peptide synthetases, in non-ribosomal peptide biosynthesis in *Bacillus subtilis*. *Arch. Microbiol. 169*, 404–410.
10. Reimmann, C., Patel, H. M., Walsh, C. T., and Haas, D. (2004) PchC thioesterase optimizes nonribosomal biosynthesis of the peptide siderophore pyochelin in *Pseudomonas aeruginosa*. *J. Bacteriol. 186*, 6367–6373.
11. Geoffroy, V. A., Fetherston, J. D., and Perry, R. D. (2000) *Yersinia pestis* YbtU and YbtT are involved in synthesis of the siderophore

yersiniabactin but have different effects on regulation. *Infect. Immun. 68*, 4452–4461.
12. Leduc, D., Battesti, A., and Bouveret, E. (2007) The hotdog thioesterase EntH (YbdB) plays a role in vivo in optimal enterobactin biosynthesis by interacting with the ArCP domain of EntB. *J. Bacteriol. 189*, 7112–7126.
13. Kim, B. S., Cropp, T. A., Beck, B. J., Sherman, D. H., and Reynolds, K. A. (2002) Biochemical evidence for an editing role of thioesterase II in the biosynthesis of the polyketide pikromycin. *J. Biol. Chem. 277*, 48028–48034.
14. Crosa, J. H., and Walsh, C. T. (2002) Genetics and assembly line enzymology of siderophore biosynthesis in bacteria. *Microbiol. Mol. Biol. Rev. 66*, 223–249.
15. Gehring, A. M., Mori, I., and Walsh, C. T. (1998) Reconstitution and characterization of the Escherichia coli enterobactin synthetase from EntB, EntE, and EntF. *Biochemistry 37*, 2648–2659.
16. Rusnak, F., Faraci, W. S., and Walsh, C. T. (1989) Subcloning, expression, and purification of the enterobactin biosynthetic enzyme 2,3-dihydroxybenzoate-AMP ligase: demonstration of enzyme-bound (2, 3-dihydroxybenzoyl) adenylate product. *Biochemistry 28*, 6827–6835.
17. Gehring, A. M., Bradley, K. A., and Walsh, C. T. (1997) Enterobactin biosynthesis in *Escherichia coli*: isochorismate lyase (EntB) is a bifunctional enzyme that is phosphopantetheinylated by EntD and then acylated by EntE using ATP and 2,3-dihydroxybenzoate. *Biochemistry 36*, 8495–8503.
18. Shaw-Reid, C. A., Kelleher, N. L., Losey, H. C., Gehring, A. M., Berg, C., and Walsh, C. T. (1999) Assembly line enzymology by multimodular nonribosomal peptide synthetases: the thioesterase domain of *E. coli* EntF catalyzes both elongation and cyclolactonization. *Chem. Biol. 6*, 385–400.
19. Roche, E. D., and Walsh, C. T. (2003) Dissection of the EntF condensation domain boundary and active site residues in nonribosomal peptide synthesis. *Biochemistry 42*, 1334–1344.
20. Badger, J., Sauder, J. M., Adams, J. M., Antonysamy, S., Bain, K., Bergseid, M. G., Buchanan, S. G., Buchanan, M. D., Batiyenko, Y., Christopher, J. A., Emtage, S., Eroshkina, A., Feil, I., Furlong, E. B., Gajiwala, K. S., Gao, X., He, D., Hendle, J., Huber, A., Hoda, K., Kearins, P., Kissinger, C., Laubert, B., Lewis, H. A., Lin, J., Loomis, K., Lorimer, D., Louie, G., Maletic, M., Marsh, C. D., Miller, I., Molinari, J., Muller-Dieckmann, H. J., Newman, J. M., Noland, B. W., Pagarigan, B., Park, F., Peat, T. S., Post, K. W., Radojicic, S., Ramos, A., Romero, R., Rutter, M. E., Sanderson, W. E., Schwinn, K. D., Tresser, J., Winhoven, J., Wright, T. A., Wu, L., Xu, J., and Harris, T. J. (2005) Structural analysis of a set of proteins resulting from a bacterial genomics project. *Proteins 60*, 787–796.
21. Leesong, M., Henderson, B. S., Gillig, J. R., Schwab, J. M., and Smith, J. L. (1996) Structure of a dehydratase-isomerase from the bacterial pathway for biosynthesis of unsaturated fatty acids: two catalytic activities in one active site. *Structure 4*, 253–264.
22. Dillon, S. C., and Bateman, A. (2004) The hotdog fold: wrapping up a superfamily of thioesterases and dehydratases. *BMC Bioinf. 5*, 109.
23. Song, F., Zhuang, Z., Finci, L., Dunaway-Mariano, D., Kniewel, R., Buglino, J. A., Solorzano, V., Wu, J., and Lima, C. D. (2006) Structure, function, and mechanism of the phenylacetate pathway hot dog-fold thioesterase PaaI. *J. Biol. Chem. 281*, 11028–11038.
24. Cheng, Z., Song, F., Shan, X., Wei, Z., Wang, Y., Dunaway-Mariano, D., and Gong, W. (2006) Crystal structure of human thioesterase superfamily member 2. *Biochem. Biophys. Res. Commun. 349*, 172–177.
25. Song, F., Zhuang, Z., and Dunaway-Mariano, D. (2007) Structure-activity analysis of base and enzyme-catalyzed 4-hydroxybenzoyl coenzyme A hydrolysis. *Bioorg. Chem. 35*, 1–10.
26. Zhuang, Z., Song, F., Zhao, H., Li, L., Cao, J., Eisenstein, E., Herzberg, O., and Dunaway-Mariano, D. (2008) Divergence of function in the hot dog fold enzyme superfamily: the bacterial thioesterase YciA. *Biochemistry 47*, 2789–2796.
27. Willis, M. A., Zhuang, Z., Song, F., Howard, A., Dunaway-Mariano, D., and Herzberg, O. (2008) Structure of YciA from *Haemophilus influenzae* (HI0827), a hexameric broad specificity acyl-coenzyme A thioesterase. *Biochemistry 47*, 2797–2805.
28. Benning, M. M., Wesenberg, G., Liu, R., Taylor, K. L., Dunaway-Mariano, D., and Holden, H. M. (1998) The three-dimensional structure of 4-hydroxybenzoyl-CoA thioesterase from *Pseudomonas* sp. strain CBS-3. *J. Biol. Chem. 273*, 33572–33579.
29. Zhuang, Z., Song, F., Zhang, W., Taylor, K., Archambault, A., Dunaway-Mariano, D., Dong, J., and Carey, P. R. (2002) Kinetic, Raman, NMR, and site-directed mutagenesis studies of the Pseudomonas sp. CBS3 4-hydroxybenzoyl-CoA thioesterase active site. *Biochemistry 41*, 11152–11160.
30. Thoden, J. B., Holden, H. M., Zhuang, Z., and Dunaway-Mariano, D. (2002) X-ray crystallographic analyses of inhibitor and substrate complexes of wild-type and mutant 4-hydroxybenzoyl-CoA thioesterase. *J. Biol. Chem. 277*, 27468–27476.
31. Thoden, J. B., Zhuang, Z., Dunaway-Mariano, D., and Holden, H. M. (2003) The structure of 4-hydroxybenzoyl-CoA thioesterase from *Arthrobacter* sp. strain SU. *J. Biol. Chem. 278*, 43709–43716.
32. Zhuang, Z., Gartemann, K. H., Eichenlaub, R., and Dunaway-Mariano, D. (2003) Characterization of the 4-hydroxybenzoyl-coenzyme A thioesterase from *Arthrobacter* sp. strain SU. *Appl. Environ. Microbiol. 69*, 2707–2711.
33. Guo, Z.-F., Jiang, M., Zheng, S., and Guo, Z. (2008) Suppression of linear side products by macromolecular crowding in nonribosomal enterobactin biosynthesis. *Org. Lett. 10*, 649–652.
34. Jiang, M., Chen, X., Guo, Z.-F., Cao, Y., Chen, M., and Guo, Z. (2008) Identification and characterization of (1*R*, 6R)-2-succinyl-6-hydroxy-2, 4-cyclohexadiene-1-carboxylate synthase in the menaquinone biosynthesis of *Escherichia coli*. *Biochemistry 47*, 3426–3434.
35. Tipton, K. F., and Dixon, H. B. (1979) Effects of pH on enzymes. *Methods Enzymol. 63*, 183–234.
36. Lai, M.-T., Li, D., Oh, E., and Liu, H.-W. (1993) Inactivation of medium-chain acyl-CoA dehydrogenase by a metabolite of hypoglycin: Characterization of the major turnover product and evidence suggesting an alternative flavin modification pathway. *J. Am. Chem. Soc. 115*, 1619–1628.
37. Holm, L., and Park, J. (2000) DaliLite workbench for protein structure comparison. *Bioinformatics 16*, 566–567.
38. Li, J., Derewenda, U., Dauter, Z., Smith, S., and Derewenda, Z. S. (2000) Crystal structure of the *Escherichia coli* thioesterase II, a homolog of the human Nef binding enzyme. *Nat. Struct. Biol. 7*, 555–559.
39. DeLano, W. L. (2002) *The PyMOL User's Manual*, DeLano Scientific, San Carlos, CA.
40. Shah, J. (2003) The salicylic acid loop in plant defense. *Curr. Opin. Plant Biol. 6*, 365–371.
41. Meganathan, R. (2001) Biosynthesis of menaquinone (Vitamin K2) and ubiquinone (Coenzyme Q): A perspective on enzymatic mechanisms. *Vitam. Horm. 61*, 173–218.
42. Lawrence, J., Cox, G. B., and Gibson, F. (1974) Biosynthesis of ubiquinone in *Escherichia coli* K-12: Biochemical and genetic characterization of a mutant unable to convert chorismate into 4-hydroxybenzoate. *J. Bacteriol. 118*, 41–45.
43. Koglin, A., Löhr, F., Bernhard, F., Rogov, V. V., Frueh, D. P., Strieter, E. R., Mofid, M. R., Güntert, P., Wagner, G., Walsh, C. T., Marahiel, M. A., and Dötsch, V. (2008) Structural basis for the selectivity of the external thioesterase of the surfactin synthetase. *Nature 454*, 907–911.

BI802165X